NIH Public Access
Author Manuscript
Dev Cell. Author manuscript; available in PMC 2015 June 09.

Published in final edited form as:
Dev Cell. 2014 June 9; 29(5): 521–533. doi:10.1016/j.devcel.2014.04.027.

A Role for Retrotransposon LINE-1 in Fetal Oocyte Attrition in Mice

Safia Malki[1], **Godfried W. van der Heijden**[1,2], **Kathryn A. O'Donnell**[3], **Sandra L. Martin**[4], and **Alex Bortvin**[1,*]

[1]Department of Embryology, Carnegie Institution for Science, Baltimore, Maryland 21218, USA

[3]Department of Molecular Biology, University of Texas Southwestern Medical Center, Dallas, TX 75390

[4]Department of Cell and Developmental Biology, University of Colorado School of Medicine, Aurora, Colorado 80045, USA

SUMMARY

Fetal oocyte attrition (FOA) is a conserved but poorly understood process of elimination of over two-thirds of meiotic prophase I (MPI) oocytes before birth. We now implicate retrotransposons LINE-1 (L1), activated during epigenetic reprogramming of the embryonic germline, in FOA in mice. We show that wild-type fetal oocytes possess differential nuclear levels of L1ORF1p, a L1-encoded protein essential for L1 ribonucleoprotein particle (L1RNP) formation and L1 retrotransposition. We demonstrate that experimental elevation of L1 expression correlates with increased MPI defects, FOA, oocyte aneuploidy and embryonic lethality. Conversely, reverse transcriptase (RT) inhibitor AZT has a profound effect on the FOA dynamics and meiotic recombination, and implicates an RT-dependent trigger in oocyte elimination in early MPI. We propose that FOA serves to select oocytes with limited L1 activity and therefore best suited for the next generation.

INTRODUCTION

Fetal oocyte attrition (FOA) is the process of elimination of ~80% of the initial pool of human oocytes by the time of birth (Baker, 1963; Kurilo, 1981). This process is not unique to humans and has been observed in primates and extensively documented in several rodent

© 2014 Elsevier Inc. All rights reserved

*Contact: bortvin@ciwemb.edu phone: 410-246-3034 FAX: 410-243-6311.
[2]Present address: Department of Obstetrics and Gynaecology, Division of Reproductive Medicine, Erasmus MC University Medical Center, Rotterdam 3015 CE, The Netherlands

Publisher's Disclaimer: This is a PDF file of an unedited manuscript that has been accepted for publication. As a service to our customers we are providing this early version of the manuscript. The manuscript will undergo copyediting, typesetting, and review of the resulting proof before it is published in its final citable form. Please note that during the production process errors may be discovered which could affect the content, and all legal disclaimers that apply to the journal pertain.

SUPPLEMENTAL INFORMATION Supplemental Information includes Supplemental Experimental Procedures, 5 Supplemental figures and 7 Supplemental tables and can be found with this article online at http://

AUTHOR CONTRIBUTIONS S.M. and A.B. conceived and designed the experiments. S.M. performed all experiments. S.M. and A.B. analyzed the data and wrote the paper. G.W.H., S.L.M. and K.A.O'D contributed expertise and reagents.

The authors declare no conflict of interests.

NIH-PA Author Manuscript
NIH-PA Author Manuscript
NIH-PA Author Manuscript

NIH-PA Author Manuscript

NIH-PA Author Manuscript

NIH-PA Author Manuscript

species (Baker, 1966; Beaumont and Mandl, 1962; Burgoyne and Baker, 1985; Ioannou, 1964; McClellan et al., 2003). In addition, oocyte loss is observed in invertebrates suggesting a possibility of ancient evolutional origin of FOA (Matova and Cooley, 2001). In mice, fetal oocyte loss occurs continuously throughout the meiotic prophase I (MPI) and appears to require, at least in part, apoptotic mechanisms (Bergeron et al., 1998; Ene et al., 2013; Ghafari et al., 2007; McClellan et al., 2003; Morita et al., 2000). However, despite the apparent evolutional conservation of FOA, questions of the molecular basis and rationale (if any) for oocyte purging remain open (Hartshorne et al., 2009). Over the years, a few scenarios have been considered but none have been firmly ruled out or confirmed experimentally to date (Tilly, 2001). These include “death by neglect”, “death by defect” and “death by self-sacrifice” that correspond to proposed roles of growth factors, meiotic checkpoints and cyst organization of the embryonic oogenesis (Barlow et al., 1998; Lei and Spradling, 2013; Morita et al., 1999; Morita et al., 2001; Pepling and Spradling, 2001).

Over the past decade, DNA methylation remodeling of the embryonic germline has become recognized as an important aspect of germ cell development and differentiation (Lees-Murdock and Walsh, 2008; Popp et al., 2010; Seisenberger et al., 2012). The erasure of repressive DNA methylation creates a window of opportunity for expression of transposable elements (TEs) whose intact and mutated copies constitute ~40% of the mouse genome (Bourc'his and Bestor, 2004; Hajkova et al., 2002; Walsh et al., 1998; Waterston et al., 2002). At least two mechanisms, DNA methylation and PIWI-interacting RNAs (piRNAs), are required to efficiently silence TEs *de novo* (Aravin and Bourc'his, 2008; Bourc'his and Bestor, 2004). Studies of mouse mutants lacking piRNAs demonstrated the essential role of these small RNAs in transcriptional and post-transcriptional transposon control (Aravin et al., 2008; Kuramochi-Miyagawa et al., 2008). Interestingly, upregulation of transposons is particularly detrimental to MPI male germ cells (Aravin et al., 2009; Carmell et al., 2007; Ollinger et al., 2010; Shoji et al., 2009; Soper et al., 2008). This observation is important since the onset of DNA methylation reprogramming and transposon derepression just precede sex determination of primordial germ cells, which is manifested as the cell-cycle arrest of prospermatogonia and the meiotic entry of oocytes (Seisenberger et al., 2012; Western, 2009). Therefore, by analogy with lethality of piRNA- or DNA methylation-deficient spermatocytes, massive elimination of fetal oocytes could be a product of the concurrency of transposon derepression and meiotic initiation (Figure 1A). While none of the reported mouse mutants lacking piRNA machinery have been described to exhibit female infertility, a prior study linked extensive global DNA demethylation in the *Hells/LSH* mutant with MPI defects and derepression of IAP elements, which otherwise elude extensive DNA methylation reprogramming (De La Fuente et al., 2006; Lane et al., 2003). In this work we set out to examine in details the impact of retrotransposons on viability and quality of fetal oocytes in mice.

RESULTS

Mutation of *Mael* Increases L1 Expression and Enhances Fetal Oocyte Attrition

We reasoned that expression of transposable elements throughout MPI could contribute to FOA (Figure 1A). To begin to test this hypothesis, we first used immunofluorescence to

NIH-PA Author Manuscript

NIH-PA Author Manuscript

NIH-PA Author Manuscript

assess fetal oocyte expression of two classes of retrotransposons active in the mouse genome - non-LTR retrotransposons L1 and endogenous retroviruses IAP (Goodier and Kazazian, 2008). Based on immunostaining for L1ORF1p, a L1-encoded protein that is a component of L1 ribonucleoprotein particles (L1RNPs) with an essential role in L1 retrotransposition (Doucet et al., 2010; Martin, 2006; Martin et al., 2008), L1 elements were found to be expressed in all MPI oocytes of the fetal ovary (Figure 1B). In contrast, we did not detect IAP GAG protein expression until later in oogenesis (Figure S1). This is consistent with a prior report of IAPs being resistant to epigenetic reprogramming (Lane et al., 2003). Given these observations and persistence of L1 activity in the human genome (Beck et al., 2010; Brouha et al., 2003; Kazazian, 2004), we focused our subsequent studies on L1 elements.

To assess the effect of increased L1 expression on viability of fetal oocytes, we first studied mice lacking *maelstrom homolog (Drosophila)* (*Mael*) gene that encodes a protein with an evolutionarily conserved role in transposon silencing (Aravin et al., 2009; Lim and Kai, 2007; O'Donnell et al., 2008; Sienski et al., 2012; Soper et al., 2008). Using anti-MAEL antibodies (Soper et al., 2008), we detected MAEL expression in fetal oocytes, primordial and primary follicles (Figures 2A–2F). *Mael*-null embryonic day 15.5 (E15.5) ovaries contained a 2.3- and 2.4-fold excess of L1 mRNA and L1ORF1p, respectively, above levels already present in the wild type (WT) (Figures 2G–2I). RNA-Seq analysis of WT and *Mael*-null E15.5 ovaries revealed abundant expression of L1 elements of active families and their 2-fold increase in the *Mael* mutant (Figure S2A). We also observed increased expression of genes associated with cell death and transcripts from contaminating hematopoietic cells but did not see altered expression of genes with established roles in germ cells or meiosis (Figure S2B, Table S1 and Experimental Procedures).

To evaluate the effect of the *Mael* mutation on FOA, we quantified oocytes in E15.5, E18.5 and postnatal day 2 (P2) WT and *Mael*-mutant ovaries. At E15.5, when all oocytes have entered MPI, ovaries of both genotypes had comparable oocyte numbers (Figure 3A, Tables S2A and S2B). However, of the initial WT and *Mael*-null E15.5 populations, only 55% and 18% survived to E18.5, and 40% and 14% to P2, respectively (Figure 3A, Tables S2A and S2B). Therefore, upregulation of L1 expression in *Mael*-null fetal oocytes correlated with their reduced viability.

Differential Accumulation of L1ORF1p in Fetal Oocyte Nuclei

We next wanted to understand how widespread derepression of L1 expression in the female germline could lead to elimination of not all but only a subpopulation of fetal oocytes. Since L1 must reach the oocyte genome to retrotranspose and cause DNA damage during this process (Belgnaoui et al., 2006; Gasior et al., 2006; Soper et al., 2008), we examined nuclear levels of L1ORF1p, an RNA-binding chaperone protein and essential component of L1RNPs (Martin, 2006; Martin et al., 2008; Martin et al., 2005), in fetal oocytes. Unexpectedly, we observed that oocytes of the same age and genotype exhibited significant variation of nuclear levels of L1ORF1p immunofluorescence (Figure 3B). To further characterize this variation, we developed an approach to determine relative mean nuclear (RMN) L1ORF1p levels in individual fetal oocytes (Figure 3C and Experimental Procedures). Using this approach, we quantified nuclear L1ORF1p levels in WT and *Mael*-

NIH-PA Author Manuscript

NIH-PA Author Manuscript

NIH-PA Author Manuscript

null E15.5, E18.5 and P2 oocytes (Figure 3D, Tables S2C and S2D). This analysis revealed broad ranges of nuclear L1ORF1p accumulation even in the starting population of WT and *Mael*-null E15.5 oocytes with maximum values of 6.62 and 7.92 RMN units, respectively. In surviving WT E18.5 oocytes (55% of the starting E15.5 population), L1ORF1p levels peaked 8.7 RMN units compared to the maximum of 9.0 RMN units in *Mael*-null oocytes that survived to E18.5 (18% of the starting E15.5 population). Despite comparable ranges of L1ORF1p nuclear accumulation between the two genotypes, statistical analysis established that *Mael*-null E15.5 and E18.5 oocyte populations were distinct from their respective WT counterparts and contained more oocytes with higher nuclear L1ORF1p levels (Tables S2C and S2D). By P2, however, the maximum nuclear L1ORF1p level in WT oocytes (40% of the starting E15.5 population) decreased to 3.13 RMN units. In contrast, L1ORF1p levels remained high in viable *Mael*-null P2 oocytes (14% of the starting E15.5 population). These results established that WT and *Mael*-mutant fetal and early postnatal ovaries contained highly heterogeneous populations of MPI oocytes characterized by differential and dynamic accumulation of L1ORF1p in their nuclei.

The unexpected variation of L1ORF1p levels as early as E15.5 could arise from any combination of differential DNA demethylation and derepression of 11,000 full-length L1 elements in the mouse genome (Goodier et al., 2001) or asynchronous onset of epigenetic reprogramming. To reconcile oocyte viability data with differential L1ORF1p nuclear accumulation in both genotypes, we hypothesized that the developmental fate of a fetal oocyte (survival *versus* elimination) could be determined by its nuclear L1 content. This idea is based on prior evidence of increased DNA damage and meiotic defects following L1 activation (Belgnaoui et al., 2006; Gasior et al., 2006; Soper et al., 2008) and increased L1 expression and FOA in the absence of *Mael* (Figures 2G–I and 3A). A simplest scenario was that L1ORF1p nuclear levels (hence L1 activity) in an E15.5 oocyte determine the probability of its survival to E18.5 or P2. To test this model, we ranked E15.5 oocytes of both genotypes (representing starting oocyte populations) according to their RMN L1ORF1p values and intersected percent survival of E15.5 oocytes to E18.5 and P2 with corresponding RMN L1ORF1p curves (Figure 3E and 3F). This operation identified close maximum RMN values for WT and *Mael*-null oocytes corresponding to their survival to E18.5 (1.62 and 1.49 RMN units, respectively) and P2 (1.42 and 1.35 RMN units, respectively). This analysis suggested that WT and *Mael*-null E15.5 oocytes with L1ORF1p levels above the threshold of 1.6 RMN units were first to accumulate lethal levels of L1 activity before E18.5 while E15.5 oocytes with RMN L1ORF1p values from 1.35 to 1.6 units survived past E18.5 but were killed by P2. This analysis strongly supported our working hypothesis that L1 could play a role in FOA by causing elimination of oocytes with excessive L1 activity. Furthermore, in agreement with prior studies of L1 derepression on meiotic cells, this analysis predicted the appearance of non-meiotic DNA double-stranded breaks (DSBs) in WT fetal oocytes and increased incidence of meiotic defects in *Mael*-null fetal oocytes overexpressing L1.

Non-meiotic DNA Double-stranded Breaks in WT Fetal Oocytes

We have previously shown that derepression of L1 elements is accompanied by the appearance of SPO11-independent, non-meiotic DSBs (Romanienko and Camerini-Otero,

NIH-PA Author Manuscript

NIH-PA Author Manuscript

NIH-PA Author Manuscript

2000; Soper et al., 2008). By analogy with spermatocytes lacking L1 silencing, our observations made in fetal oocytes led us to test the prediction that *Spo11*-null but otherwise WT fetal oocytes should possess non-meiotic DSBs. Indeed, antibodies to RAD51 recombinase, a RecA homolog, revealed that 38% of E16.5 *Spo11*-null oocytes contained RAD51 foci indicative of non-meiotic DSBs (Figure 4A and 4B) (Moens et al., 1997). A majority of RAD51-positive oocytes (32% of all oocytes scored) possessed fewer than 9 RAD51 foci while 6% of oocytes contained numerous DSBs (Figure 4B). The presence of *Spo11*-independent DNA breaks in fetal oocytes, independently observed recently by others (Carofiglio et al., 2013), strongly supports our working hypothesis of a role for L1 elements in FOA.

DNA Damage and Asynapsis in *Mael*-null Oocytes

We next assessed the impact of the *Mael* deletion (hence associated L1 overexpression) on MPI. We first compared the distribution of MPI substages in WT and *Mael*-null E18.5 ovaries and concluded that the *Mael* mutation did not alter the progression of MPI (Figure S3A and Table S3). Labeling of nuclear spreads of E18.5 pachytene oocytes for γH2AX, a marker of double-stranded breaks (DSBs) and unpaired meiotic chromatin, (Turner et al., 2005) identified that 42.8% of *Mael*-null oocytes harbored such defects compared to 16.8% in the WT (Figure 4C and Table S4A). Antibodies to RAD51 revealed unrepaired DSBs in 35.6% of *Mael*-null compared to 12.8% of WT oocytes (Figure 4C and Table S4A). Co-staining for synaptonemal complex markers SYCP1 and SYCP2 revealed incomplete homologous chromosome synapsis in 37.4% of *Mael*-null E18.5 oocytes compared to 8.3% in the wild-type (Yang and Wang, 2009) (Figure 4C and Table S4A). We also labeled fetal oocytes for BRCA1, a component of the synapsis quality control mechanism known as meiotic silencing of unpaired chromatin (MSUC) (Ichijima et al., 2011; Mahadevaiah et al., 2008; Schimenti, 2005; Turner, 2007; Turner et al., 2004; Turner et al., 2005). This analysis allows positive identification of even small areas of chromosome asynapsis but is limited to oocytes with asynapsis of fewer than two or three homologous chromosomes (Kouznetsova et al., 2009). This analysis revealed MSUC in 18.2% of WT E18.5 oocytes suggesting the presence of small areas of asynapsis that could not be reliably identified by SYCP1/SYCP2 co-staining (Figure 4C, S3C–S3F and Table S4A). In the *Mael* mutant, BRCA1 antibody labeled 32.4% of E18.5 oocytes which when compared to SYCP1/SYCP2 staining suggested a higher extent of asynapsis in the presence of elevated L1 expression (Figures 4C and S3C–S3F, and Table S4A). Overall, this analysis demonstrated that up to 18% of WT and 40% of *Mael*-null E18.5 oocytes possessed clear evidence of meiotic defects including unrepaired DSBs and asynapsis, known as primary triggers for oocyte elimination during the perinatal and early postnatal period (Di Giacomo et al., 2005).

Consistent with DNA damage- and asynapsis-activated oocyte loss during the perinatal period, the number of primordial follicles was severely reduced in P19 *Mael*-null ovaries (Figure 4D and Table S4B) (Di Giacomo et al., 2005). Furthermore, we did not observe signs of folliculogenesis in ovaries of 1 year-old mice (Figure 4E). Thus, increased L1 expression in *Mael*-mutant fetal oocytes is associated with extensive DNA damage, MPI defects, a severely reduced ovarian follicle reserve and shortened female reproductive lifespan.

NIH-PA Author Manuscript

NIH-PA Author Manuscript

NIH-PA Author Manuscript

Crossover and Meiotic Chromosome Segregation Defects in *Mael*-null Oocytes

A crucial outcome of MPI is the formation of crossovers that are essential for the precise meiotic chromosome segregation. To assess the effect of the *Mael* mutation and associated increased L1 expression on crossover formation, we examined the localization of mismatch repair protein MLH1 normally recruited to 1–3 foci on each synaptonemal complex (Baker et al., 1996). Unexpectedly, we found that 97% of all *Mael*-null pachytene E18.5 oocytes with fully synapsed homologous chromosomes were lacking MLH1 foci on at least one chromosome bivalent (Figures 5A, 5D, S4A–S4C, Tables S4A, S4C and S4D). This defect could not be attributed to reduced *Mlh1* mRNA and protein levels (Figure S4E–S4G). Consistent with this finding, 70% of metaphase I *Mael*-null oocytes possessed univalent chromosomes (Figure 5B and 5D, and Table S4A) while the remaining 30% mutant oocytes exhibited a significant reduction of the average number of chiasmata per oocyte (20.9±1.7 compared to 23.4±1.5 in the WT) (Table S4C). Among ovulated metaphase II *Mael*-null oocytes, 60% had abnormal karyotypes (Figure 5C and 5D, and Table S4A) and their fertilization with WT sperm resulted in 52.5% embryonic aneuploidy at the 2-cell stage (Figure 5E and 5F, and Table S5A, and 57% lethality before the blastocyst stage (Figure 5G and Table S5B). These observations suggest that elevated L1 expression might interfere with crossover formation leading to meiotic chromosome segregation errors in the adult ovary.

Conditional Expression of a L1 Element *ORFeus* Enhances Fetal Oocyte Attrition and Meiotic Defects

We next asked if *Mael*-mutant phenotypes could be reproduced by directly increasing L1 expression in fetal oocytes. To substantially increase L1 expression over an already high background level of expression of an as many as 11,000 full-length endogenous L1 elements in the mouse genome (Goodier et al., 2001) (Figure 1B), we used a recently described mouse transgene carrying a tetracycline-controlled L1 element (*ORFeus*) (Figure 6A) (O'Donnell et al., 2013). Consistent with our earlier results, doxycycline-induced CMV-rtTA/+; tet-*ORFeus*/+ (FVBB6F1) fetal ovaries contained 14 and 13 percentage points fewer oocytes at E18.5 and P2, respectively, compared to the control group comprising non-double transgenic littermates (Figure 6B, Tables S6A–S6C and Experimental Procedures). Quantification of L1ORF1p revealed the appearance of E15.5 CMV-rtTA/+; tet-*ORFeus*/+ oocytes with increased nuclear levels of the protein that peaked at E18.5 but become depleted by P2 (Figure 6C, Tables S6D and S6E). Despite a potentially slight delay in the onset of *ORFeus* expression, RMN L1ORF1p values in the E15.5 control and double transgenic populations were nonetheless significantly distinct to reveal a correlation between the survival of E15.5 oocytes to E18.5 and P2 with their nuclear L1ORF1p levels (Figure 6D and 6E).

To assess the effect of *ORFeus* overexpression on MPI, we first compared the distribution of MPI substages in doxycycline-induced control and CMV-rtTA/+; tet-*ORFeus*/+ E18.5 ovaries and determined that *ORFeus* overexpression did not alter the MPI progression (Figure S3B). We next examined both groups of E18.5 oocytes for the presence of MPI defects. Consistent with prior results of others (Koehler et al., 2006), we observed an increased baseline level of meiotic defects in oocytes of mixed genetic background. Nevertheless, doxycycline-induced E18.5 CMV-rtTA/+; tet-*ORFeus*/+ oocytes still

NIH-PA Author Manuscript

NIH-PA Author Manuscript

NIH-PA Author Manuscript

accumulated RMN L1ORF1p levels sufficient to further increase DNA damage and chromosome asynapsis in oocytes surviving to E18.5 (Figure 6F and Table S6F). Subsequent labeling of E18.5 CMV-rtTA/+; tet-*ORFeus*/+ oocytes for BRCA1 suggested that *ORFeus* overexpression caused extensive chromosome asynapsis as indicated by a lower percent of MSUC-positive oocytes (9.4%) compared to 19% of asynapsed oocytes as determined by SYCP2 staining (Figure 6F and Table S6F). At the same time, *ORFeus* overexpression did not cause a statistically significant increase of oocytes lacking MLH1 foci on at least one chromosome bivalent (Figure 6F, Tables S6F and S6G). Perhaps the mechanism underlying the inhibitory effect of L1 on MLH1 localization to prospective crossover sites requires stronger L1 expression than offered by a single *ORFeus* transgene. Nonetheless, considered as a whole, the analysis showed that direct overexpression of a single L1 element in the fetal ovary had substantially enhanced oocyte elimination and reinforced the idea that L1 activity contributes to FOA.

Reverse Transcriptase Inhibitor AZT Alters Dynamics of Fetal Oocyte Attrition

To test the key prediction of our working hypothesis that inhibition of L1 activity should reduce FOA, we administered pregnant female mice with azidothymidine (AZT), a nucleoside analog inhibitor of reverse transcriptases (RTs) including L1ORF2p, which has independent RT and endonuclease activities (Dai et al., 2011; Feng et al., 1996; Jones et al., 2008) (Figure 7A). We first determined that AZT treatment did not perturb MPI progression or induce oocyte proliferation (Figures S3A and S5). Quantification of the oocyte content of AZT-treated WT and *Mael*-null ovaries revealed a profound yet complex effect of the drug on oocyte viability (Figure 7B, Tables S7A–S7C). In contrast to untreated controls, AZT-treated WT E18.5 ovaries retained practically an entire starting oocyte population (96%). Likewise, 61% of the starting oocyte population survived in the AZT-treated E18.5 *Mael*-mutant ovaries. The effect of AZT on E18.5 oocyte survival was sufficiently robust to be apparent in whole-mount oocyte staining of WT and *Mael*-null E18.5 ovaries (Figure 7C). This result strongly supported the idea of a role of L1 in FOA and suggested that an RT-dependent intermediate or step during L1 retrotransposition triggers oocyte elimination in the early MPI (E15.5 – E18.5), before the engagement of checkpoints monitoring the completion of meiotic DNA recombination and synapsis starting at E18.5.

Quantification of L1ORF1p immunofluorescence in AZT-treated WT and *Mael*-null E18.5 oocytes revealed the presence of predicted but previously undetected oocytes with L1ORF1p levels greatly exceeding those observed in untreated ovaries (Figure 7D, Tables S7D–S7F). L1ORF1p nuclear levels peaked at 20.7 and 36.8 RMN units in AZT-treated WT and *Mael*-null E18.5 oocytes, respectively. Since practically all AZT-treated WT oocytes survived to E18.5, L1ORF1p nuclear accumulation in WT fetal oocytes has a maximum of about 20 RMN units. In light of this data and an up to 2.4-fold increase in L1 expression levels in the *Mael*-null ovaries (Figure 2D–2I), AZT-treated *Mael*-null oocytes should have peaked at 46 RMN units but in reality did not exceed the maximum of 36.8 RMN units. Most likely, the concentration of AZT used in our experiments (5mg/kg/day) was insufficient to block RT in *Mael*-null oocytes with most L1 expression resulting in elimination of 39% of the starting oocyte population. Taken together, these observations support the idea of preferential elimination of fetal oocytes with excessive levels of nuclear L1ORF1p during FOA.

NIH-PA Author Manuscript

NIH-PA Author Manuscript

NIH-PA Author Manuscript

Despite the strong protective effect of AZT on early (E15.5–E18.5) MPI oocytes, we found that AZT-treated WT and *Mael*-mutant P2 ovaries contained 41% and 31% of the starting oocyte populations, respectively. A sharp drop in oocyte viability was not unexpected as AZT does inhibit the endonuclease activity of L1ORF2p. Up to 40% of AZT-treated WT E18.5 oocytes exhibited MPI defects, which is consistent with the percent of eliminated E18.5 oocytes in untreated WT ovaries (Figure 7E, Tables S7G and S7H). Likewise, in addition to 39% of *Mael*-null oocytes eliminated by E18.5, up to 37% of AZT-treated E18.5 oocytes possessed elevated DNA damage and asynapsis. These defects were the likely triggers of checkpoint activation and a sharp decline in oocyte numbers in the early postnatal period (Figure 7B, Tables S7A and S7B) (Di Giacomo et al., 2005).

Finally, we examined the effect of AZT treatment on the number and distribution of MLH1 foci. In a stark contrast to untreated *Mael*-null E18.5 oocytes 97% of which lacked MLH1 foci on at least one chromosome bivalent, we found that only 28.9% of AZT treated *Mael*-null E18.5 oocytes exhibited such a defect (Figure 7E, Tables S7G–S7J). The mean number of MLH1 foci in *Mael*-null E18.5 oocytes increased from 9.97±5.32 without treatment to 22.76±6.24 in the presence of AZT (Figure S5 and Table S7I). Furthermore, quantification of MLH1 foci in AZT-treated E18.5 WT oocytes revealed a statistically significant increase in the mean number of MLH1 foci from 26.55±5.94 to 28.83±4.9 (Figure S5 and Tables S7I, S7J). These findings suggest that an RT-dependent intermediate of L1 retrotransposition interferes with crossover formation not only in the absence of *Mael* but also under basal conditions of L1 expression in WT MPI oocytes.

Considered as a whole, the results of analysis of WT and *Mael*-mutant ovaries treated with AZT are highly consistent with the hypothesis that L1 activity plays a role in FOA and suggest that intermediates of L1 retrotransposition such as L1 RNA-DNA hybrids might trigger elimination of early MPI oocytes.

DISCUSSION

In this work, we examined a role of retrotransposon L1 in FOA in mice. We reasoned that expression of L1 elements following their activation in the course of epigenetic reprogramming could be detrimental to viability of MPI fetal oocytes. We have uncovered differential accumulation of nuclear L1ORF1p, hence L1RNPs, among WT fetal oocytes. By studying fetal oocytes of WT and L1-overexpressing mice we were able to establish a correlation between fetal oocyte nuclear L1ORF1p levels and oocyte viability. We used two different strategies to increase L1 expression in fetal oocytes to assess if high levels of L1 associate with enhanced MPI defects and oocyte elimination. A null mutation in the *Mael* gene allowed an up to 2.4-fold increase in global L1 expression which resulted in a 3-fold reduction in the number of fetal oocytes at birth. Induction of expression of a single L1 element *ORFeus* at the onset of MPI has also resulted in reduced oocyte survival which can be correlated with nuclear L1ORF1p levels. While not as strong as the *Mael*-mutant phenotype, the effect of *ORFeus* overexpression is quite significant especially in light of the fact that the mouse genome is estimated to encode 11,000 full-length L1 elements (Goodier et al., 2001). A central role of L1 in FOA is also strongly supported by results of experiments using RT inhibitor AZT whose administration had an immediate positive effect

NIH-PA Author Manuscript

NIH-PA Author Manuscript

NIH-PA Author Manuscript

on the dynamics of FOA in WT and *Mael*-mutant ovaries. Furthermore, AZT treatment caused a 3-fold increase in the number of *Mael*-null oocytes with normal localization of MLH1 protein to prospective crossover sites. Overall, our data support the "death by defect" model of FOA (Tilly, 2001) with both reverse transcriptase and endonuclease activities of L1ORF2p contributing to oocyte elimination. AZT-dependent protection of oocytes during early MPI (E15.5–E18.5) suggests that L1 RNA-DNA hybrids, formed in the process of target-primed retrotransposition of L1 elements, could trigger FOA. This unexpected finding and the presence of non-meiotic DSBs agree with an earlier observation that both domains of L1ORF2p contributed individually to cytotoxicity of expression of human L1 element in HeLa cells (Wallace et al., 2008).

Our work has yielded two additional significant findings. First, we observed differential nuclear accumulation of L1ORF1p among otherwise genetically identical oocytes including in the wild type. The mechanism behind this observation remains to be elucidated. Perhaps the onset or extent of DNA demethylation of the mouse genome varies between individual primordial germ cells and MPI oocytes leading to differential expression of L1 elements (Kagiwada et al., 2013; Ohno et al., 2013). L1 mobilization during early embryogenesis might also lead to a greater diversity of genotypes than had been anticipated previously (Kano et al., 2009). Second, our data suggest that L1 activity in fetal oocytes might contribute to meiotic chromosome segregation errors in the adult ovary. The mechanism of this phenomenon is not yet clear but the rescue of the MLH1 localization defect by AZT implicates newly synthesized L1 cDNA or RNA-DNA intermediates in this process, perhaps by diverting mismatch repair machinery from sites of prospective crossovers to numerous sites of L1 insertions spread throughout the genome. This observation suggests that the maternal bias of meiotic chromosome segregation errors might arise from the concurrency of developmental timing of MPI and epigenetic reprogramming in fetal oocytes. Considered together, our results lead us to conclude that L1 activity could be a potent determinant of both the size and quality of a mammalian ovarian oocyte reserve.

Finally, with respect to the rationale behind the massive loss of oocytes, we propose that FOA selects oocytes with low L1 activity and, therefore, best suited for the next generation. In the long run, limited exposure to L1 might result in novel L1 insertions and, therefore, negative effects of L1-driven oocyte demise might be balanced by positive effects of increased genetic diversity.

EXPERIMENTAL PROCEDURES

Animals

ES cell targeting, *Mael*-mutant mice derivation, backcross to C57BL/6J genetic background for >10 generations and genotyping were described previously (Soper et al., 2008). *Spo11* mutant mice were the gift of Dr. Camerini-Otero (NIDDK) (Romanienko and Camerini-Otero, 2000). Transgenic CMVrtTA/+ females in FVB genetic background (kindly provided by H.Varmus) (Sotillo et al., 2007) were mated with transgenic tet-*ORFeus*/+ males in C57BL/6J genetic background (O'Donnell et al., 2013). All experimental procedures were performed in compliance with ethical regulations and approved by the IACUC of Carnegie Institution for Science.

NIH-PA Author Manuscript

NIH-PA Author Manuscript

NIH-PA Author Manuscript

Oocyte and follicle counting

We scored all oocytes present in every fifth cryosection throughout the entire ovary. To obtain an estimate of the total number of oocytes per ovary, the numbers scored per sections was multiplied by 5 (Tilly, 2003). For statistical analysis we compared average number of oocytes per ovary counted in pairs of ovaries coming from embryos from different litters as indicated in supplemental tables (Tables S2A and S2B, S6A–S6C, S7A–S7C). To quantify follicles in postnatal ovaries, we scored follicles as “primordial” if they contained an intact oocyte with a visible nucleolus surrounded by a single layer of fusiform-shaped granulosa cells. We scored follicles as “primary” if they consisted of an intact, enlarged oocyte with a visible nucleolus and a single layer of cuboidal granulosa cells. We scored follicles as “preantral/antral” if they contained an oocyte with a visible nucleolus and more than one layer of granulosa or thecal cells. For statistical analysis we compared average number of follicles per ovary counted in pairs of ovaries coming from females from different litters as indicated in supplemental tables (Table S4B).

Induced *ORFeus* expression

To induce tet-*ORFeus* expression, doxycycline hyclate (Sigma-Aldrich, Cat#:D9891) (5mg/mL in drinking water supplemented with 1% sucrose) was provided *ad libitum* in opaque bottles to 2–6 months old transgenic CMV-rtTA/+ females mated with transgenic male tet-*ORFeus*/+ starting at 12.5 days post coitum (dpc) and refreshed every 48 hours. Treated females were dissected at 15.5 or 18.5 dpc, or P2 for subsequent analysis of ovaries. The effect of *ORFeus* activation on oocyte fate were assessed by comparing embryonic ovaries from female double transgenic (CMV-rtTA/+; tet-*ORFeus*/+) with their female littermates non DOX-inducible non-double transgenics (+/+; tet-*ORFeus*/+), (CMV-rtTA/+; +/+), (+/+; +/+) (O'Donnell et al., 2013). An independent one-sample t-test (Table S6C) demonstrates that the number of oocytes did not differ between different non-double transgenic littermates.

AZT administration

To inhibit L1 reverse transcriptase in embryonic oocytes, pregnant 2–6 months old *Mael*+/− females, mated with male *Mael*+/− males, received 5mg/kg/day AZT (Sigma Aldrich, Cat#. A2169) by gavage starting at 12.5 days post coitum (dpc). Treated females were dissected at 15.5 or 18.5 dpc, or P2 for subsequent analysis of oocytes. The route and doses of AZT used in this study were based on previous reports (Dai et al., 2011; Sharpe et al., 1988; Sharpe et al., 1987; Toltzis et al., 1991).

Analysis of L1ORF1p nuclear signal

We co-immunolabelled cryosections of embryonic ovaries for L1ORF1p and germ cell marker (SYCP2 or TRA98), and counterstained with DAPI. We performed confocal imaging using SP5 confocal microscope (Leica, Exton, PA). The 3-D reconstruction of generated Z-stacked images was performed using Imaris Software (Bitplane). For each 3-D reconstructed image we determined the 3-D DAPI-rendered surfaces in individual oocyte nuclei and collected mean intensity of green signals inside surfaces, corresponding to the mean intensity of nuclear oocyte L1ORF1p signal. To eliminate the background signals, in

NIH-PA Author Manuscript

NIH-PA Author Manuscript

NIH-PA Author Manuscript

parallel to oocyte nuclei analysis, on each image we determine the 3D DAPI-rendered surfaces of 3 ovarian somatic cell nuclei (with different location on the image) and collected mean intensity of green signals inside somatic cell nuclear surfaces. For further analysis, we determined the relative mean nuclear (RMN) L1ORF1p signals of oocytes for each image by normalizing nuclear mean intensity in each examined oocyte to the average of nuclear mean intensity of L1ORF1p signal of 3 ovarian somatic nuclei from the same image. We collected RMN from at least 99 oocytes in different images of ovaries from at least 3 different embryos for each embryonic stage and genotype.

RNA-Seq analysis

We purified total RNA from E15.5 WT and *Mael*$^{-/-}$ embryonic ovaries using TRIzol (Invitrogen). We depleted total RNA samples from ribosomal RNA using the Ribo-Zero™ rRNA Removal Kit (Epicentre) accordingly to the manufacturer's instructions. rRNA removal was visually assessed by Agilent 2100 Bioanalyzer (Agilent) RNA electropherograms. Library construction, cluster generation and sequencing on HiSeq 2000 (Illumina) were performed according to manufacturer's protocols. We obtained a total of 8.2 – 8.9 x10^7 filtered 100-bp reads for each ovarian sample. We used TopHat and Cufflinks to align reads to mouse reference genome NCBI37/mm9 and to identify differentially expressed genes (Trapnell et al., 2009; Trapnell et al., 2010). To account for the relatively complex cellular composition of the fetal ovary and anticipated variation in the number of fetal oocytes between samples, we focused on two WT and two mutant samples with best Pearson's *r* correlation coefficients (Figure S2B). Transcripts with “significant” Cuffdiff scores, FPKM count ≥ 5 and a ≥ 2-fold increase in expression in all four *Mael* mutant - WT pairwise comparisons were considered reliably altered. By these criteria, only one gene (besides *Mael*) was identified as downregulated (Table S1A) and 120 genes as upregulated in *Mael*-mutant ovaries compared to WT (Table S1B). By the same criteria, no known germ-cell or meiotic genes were found to be expressed differentially.

For analysis of expression of L1 elements belonging to young L1 families, we aligned the reads to 2383 intact, full-length L1 insertions in the mouse genome from the L1Base (http://l1base.molgen.mpg.de) (Penzkofer et al., 2005; Zemojtel et al., 2007). We used Bowtie software (Langmead et al., 2009) and allowed for 2 mismatches. To account for the cellular complexity of WT and *Mael*-mutant ovaries analyzed and compared we normalized count of mapped reads to the level of expression of a germ cell marker, Mouse Vasa Homolog (MVH) and a housekeeping gene Actin beta.

Data Deposition

High throughput sequencing data have been submitted to NCBI Short Read Archive under accession number SRP040979.

Gene Ontology Analysis

Gene Ontology analysis of genes upregulated in *Mael*-null ovaries was done using GOEAST software (Tables S1C and S1D) (Zheng and Wang, 2008). GO analysis is consistent with upregulation of apoptotic genes and contamination with cells of the hematopoietic lineage.

NIH-PA Author Manuscript

NIH-PA Author Manuscript

NIH-PA Author Manuscript

Statistical Analysis

We performed all measurements independently at least in triplicate. We analyzed random sample populations from at least 3 different samples from 3 random animals. Sample size populations are indicated in Supplemental Tables. The genotyping to allocate animals to different experimental groups were performed after sample processing. The random sample size populations used in our analyses are representative of the entire population with a 90 to 95% confidence interval and 95% confidence level (Creative Research Systems survey software http://www.surveysystem.com/sscalc.htm). Scoring of samples for analyses of meiotic prophase I progression were performed with blinding genotypes. We assessed differences between quantitative variables for normal populations of small and large sizes with the two-tailed unpaired Student's t-test (Figure 2G and 2I, Tables S2B, S4B, S4C, S4D, S5A, S5B, S6B, S6C, S6G, S7B, S7C, S7I, S7J) and with the one-sample t-test (Table S6C) (QuickCalcs http://www.graphpad.com/quickcalcs/index.cfm); two-tailed Kolmogorov-Smirnov test for non-normal populations of large size (Tables S2D, S6E, S7E, S7F) (http://www.physics.csbsju.edu). We assessed qualitative variables with two-tailed Fisher's exact test of populations of small and large sizes (Tables S4A, S5B, S6F, S7G, S7H) and chi-square test (Table S3B) (QuickCalcs http://www.graphpad.com/quickcalcs/index.cfm). Throughout the report statistical significance is indicated as (*) for $p<0.05$, (**) for $p<0.01$, (***) for $p<0.001$ and (ns) for $p>0.05$.

Details of the other standard methods and reagents are described in the Supplemental Experimental Procedures.

Supplementary Material

Refer to Web version on PubMed Central for supplementary material.

Acknowledgments

We thank M. Halpern for manuscript critique, N. Ingolia, A. Pinder and F. Tan for RNA-Seq assistance; D. Camerini-Otero for *Spo11* mice, P.J. Wang, B.R. Cullen, and R. Kanaar for antibodies. The work was supported by the endowment of Carnegie Institution for Science, by a CPRIT R1101 Award (K.A.O'D) and by the NIH grant GM40367 (S.L.M.). S.M. was a recipient of the EMBO long-term (ALTF 543-2006) and McClintock fellowships. G.W.H. was a recipient of Hollaender fellowship.

REFERENCES

Aravin AA, Bourc'his D. Small RNA guides for de novo DNA methylation in mammalian germ cells. Genes Dev. 2008; 22:970–975. [PubMed: 18413711]

Aravin AA, Sachidanandam R, Bourc'his D, Schaefer C, Pezic D, Toth KF, Bestor T, Hannon GJ. A piRNA pathway primed by individual transposons is linked to de novo DNA methylation in mice. Molecular cell. 2008; 31:785–799. [PubMed: 18922463]

Aravin AA, van der Heijden GW, Castaneda J, Vagin VV, Hannon GJ, Bortvin A. Cytoplasmic compartmentalization of the fetal piRNA pathway in mice. PLoS Genet. 2009; 5:e1000764. [PubMed: 20011505]

Baker SM, Plug AW, Prolla TA, Bronner CE, Harris AC, Yao X, Christie DM, Monell C, Arnheim N, Bradley A, et al. Involvement of mouse Mlh1 in DNA mismatch repair and meiotic crossing over. Nat Genet. 1996; 13:336–342. [PubMed: 8673133]

Baker TG. A Quantitative and Cytological Study of Germ Cells in Human Ovaries. Proc R Soc Lond B Biol Sci. 1963; 158:417–433. [PubMed: 14070052]

NIH-PA Author Manuscript

NIH-PA Author Manuscript

NIH-PA Author Manuscript

Baker TG. A quantitative and cytological study of oogenesis in the rhesus monkey. Journal of anatomy. 1966; 100:761–776. [PubMed: 4961727]

Barlow C, Liyanage M, Moens PB, Tarsounas M, Nagashima K, Brown K, Rottinghaus S, Jackson SP, Tagle D, Ried T, et al. Atm deficiency results in severe meiotic disruption as early as leptonema of prophase I. Development. 1998; 125:4007–4017. [PubMed: 9735362]

Beaumont HM, Mandl AM. A quantitative and cytological study of oognonia and oocytes in the foetal and nonatal rat. Proc R Soc Lond B Biol Sci. 1962; 155:557–579.

Beck CR, Collier P, Macfarlane C, Malig M, Kidd JM, Eichler EE, Badge RM, Moran JV. LINE-1 retrotransposition activity in human genomes. Cell. 2010; 141:1159–1170. [PubMed: 20602998]

Belgnaoui SM, Gosden RG, Semmes OJ, Haoudi A. Human LINE-1 retrotransposon induces DNA damage and apoptosis in cancer cells. Cancer Cell Int. 2006; 6:13. [PubMed: 16670018]

Bergeron L, Perez GI, Macdonald G, Shi L, Sun Y, Jurisicova A, Varmuza S, Latham KE, Flaws JA, Salter JC, et al. Defects in regulation of apoptosis in caspase-2-deficient mice. Genes & development. 1998; 12:1304–1314. [PubMed: 9573047]

Bourc'his D, Bestor TH. Meiotic catastrophe and retrotransposon reactivation in male germ cells lacking Dnmt3L. Nature. 2004; 431:96–99. [PubMed: 15318244]

Brouha B, Schustak J, Badge RM, Lutz-Prigge S, Farley AH, Moran JV, Kazazian HH Jr. Hot L1s account for the bulk of retrotransposition in the human population. Proceedings of the National Academy of Sciences of the United States of America. 2003; 100:5280–5285. [PubMed: 12682288]

Burgoyne PS, Baker TG. Perinatal oocyte loss in XO mice and its implications for the aetiology of gonadal dysgenesis in XO women. J Reprod Fertil. 1985; 75:633–645. [PubMed: 3906118]

Carmell MA, Girard A, van de Kant HJ, Bourc'his D, Bestor TH, de Rooij DG, Hannon GJ. MIWI2 is essential for spermatogenesis and repression of transposons in the mouse male germline. Dev Cell. 2007; 12:503–514. [PubMed: 17395546]

Carofiglio F, Inagaki A, de Vries S, Wassenaar E, Schoenmakers S, Vermeulen C, van Cappellen WA, Sleddens-Linkels E, Grootegoed JA, Te Riele HP, et al. SPO11-independent DNA repair foci and their role in meiotic silencing. PLoS genetics. 2013; 9:e1003538. [PubMed: 23754961]

Dai L, Huang Q, Boeke JD. Effect of reverse transcriptase inhibitors on LINE-1 and Ty1 reverse transcriptase activities and on LINE-1 retrotransposition. BMC Biochem. 2011; 12:18. [PubMed: 21545744]

De La Fuente R, Baumann C, Fan T, Schmidtmann A, Dobrinski I, Muegge K. Lsh is required for meiotic chromosome synapsis and retrotransposon silencing in female germ cells. Nat Cell Biol. 2006; 8:1448–1454. [PubMed: 17115026]

Di Giacomo M, Barchi M, Baudat F, Edelmann W, Keeney S, Jasin M. Distinct DNA-damage-dependent and -independent responses drive the loss of oocytes in recombination-defective mouse mutants. Proc Natl Acad Sci U S A. 2005; 102:737–742. [PubMed: 15640358]

Doucet AJ, Hulme AE, Sahinovic E, Kulpa DA, Moldovan JB, Kopera HC, Athanikar JN, Hasnaoui M, Bucheton A, Moran JV, et al. Characterization of LINE-1 ribonucleoprotein particles. PLoS genetics. 2010; 6

Ene AC, Park S, Edelmann W, Taketo T. Caspase 9 is constitutively activated in mouse oocytes and plays a key role in oocyte elimination during meiotic prophase progression. Developmental biology. 2013; 377:213–223. [PubMed: 23384561]

Feng Q, Moran JV, Kazazian HH Jr. Boeke JD. Human L1 retrotransposon encodes a conserved endonuclease required for retrotransposition. Cell. 1996; 87:905–916. [PubMed: 8945517]

Gasior SL, Wakeman TP, Xu B, Deininger PL. The human LINE-1 retrotransposon creates DNA double-strand breaks. J Mol Biol. 2006; 357:1383–1393. [PubMed: 16490214]

Ghafari F, Gutierrez CG, Hartshorne GM. Apoptosis in mouse fetal and neonatal oocytes during meiotic prophase one. BMC Dev Biol. 2007; 7:87. [PubMed: 17650311]

Goodier JL, Kazazian HH Jr. Retrotransposons revisited: the restraint and rehabilitation of parasites. Cell. 2008; 135:23–35. [PubMed: 18854152]

Goodier JL, Ostertag EM, Du K, Kazazian HH Jr. A novel active L1 retrotransposon subfamily in the mouse. Genome research. 2001; 1:1677–1685. [PubMed: 11591644]

NIH-PA Author Manuscript

NIH-PA Author Manuscript

NIH-PA Author Manuscript

Hajkova P, Erhardt S, Lane N, Haaf T, El-Maarri O, Reik W, Walter J, Surani MA. Epigenetic reprogramming in mouse primordial germ cells. Mech Dev. 2002; 117:15–23. [PubMed: 12204247]

Hartshorne GM, Lyrakou S, Hamoda H, Oloto E, Ghafari F. Oogenesis and cell death in human prenatal ovaries: what are the criteria for oocyte selection? Mol Hum Reprod. 2009; 15:805–819. [PubMed: 19584195]

Ichijima Y, Ichijima M, Lou Z, Nussenzweig A, Camerini-Otero RD, Chen J, Andreassen PR, Namekawa SH. MDC1 directs chromosome-wide silencing of the sex chromosomes in male germ cells. Genes & development. 2011; 25:959–971. [PubMed: 21536735]

Ioannou JM. Ooegenesis in the Guinea-Pig. Journal of embryology and experimental morphology. 1964; 12:673–691. [PubMed: 14251479]

Jones RB, Garrison KE, Wong JC, Duan EH, Nixon DF, Ostrowski MA. Nucleoside analogue reverse transcriptase inhibitors differentially inhibit human LINE-1 retrotransposition. PloS one. 2008; 3:e1547. [PubMed: 18253495]

Kagiwada S, Kurimoto K, Hirota T, Yamaji M, Saitou M. Replication-coupled passive DNA demethylation for the erasure of genome imprints in mice. The EMBO journal. 2013; 32:340–353. [PubMed: 23241950]

Kano H, Godoy I, Courtney C, Vetter MR, Gerton GL, Ostertag EM, Kazazian HH Jr. L1 retrotransposition occurs mainly in embryogenesis and creates somatic mosaicism. Genes Dev. 2009; 23:1303–1312. [PubMed: 19487571]

Kazazian HH Jr. Mobile elements: drivers of genome evolution. Science. 2004; 303:1626–1632. [PubMed: 15016989]

Koehler KE, Schrump SE, Cherry JP, Hassold TJ, Hunt PA. Near-human aneuploidy levels in female mice with homeologous chromosomes. Curr Biol. 2006; 16:R579–580. [PubMed: 16890511]

Kouznetsova A, Wang H, Bellani M, Camerini-Otero RD, Jessberger R, Hoog C. BRCA1-mediated chromatin silencing is limited to oocytes with a small number of asynapsed chromosomes. Journal of cell science. 2009; 122:2446–2452. [PubMed: 19531582]

Kuramochi-Miyagawa S, Watanabe T, Gotoh K, Totoki Y, Toyoda A, Ikawa M, Asada N, Kojima K, Yamaguchi Y, Ijiri TW, et al. DNA methylation of retrotransposon genes is regulated by Piwi family members MILI and MIWI2 in murine fetal testes. Genes Dev. 2008; 22:908–917. [PubMed: 18381894]

Kurilo LF. Oogenesis in antenatal development in man. Human genetics. 1981; 57:86–92. [PubMed: 7262874]

Lane N, Dean W, Erhardt S, Hajkova P, Surani A, Walter J, Reik W. Resistance of IAPs to methylation reprogramming may provide a mechanism for epigenetic inheritance in the mouse. Genesis. 2003; 35:88–93. [PubMed: 12533790]

Langmead B, Trapnell C, Pop M, Salzberg SL. Ultrafast and memory-efficient alignment of short DNA sequences to the human genome. Genome biology. 2009; 10:R25. [PubMed: 19261174]

Lees-Murdock DJ, Walsh CP. DNA methylation reprogramming in the germ line. Epigenetics. 2008; 3:5–13. [PubMed: 18259118]

Lei L, Spradling AC. Mouse primordial germ cells produce cysts that partially fragment prior to meiosis. Development. 2013; 140:2075–2081. [PubMed: 23578925]

Lim AK, Kai T. Unique germ-line organelle, nuage, functions to repress selfish genetic elements in Drosophila melanogaster. Proceedings of the National Academy of Sciences of the United States of America. 2007; 104:6714–6719. [PubMed: 17428915]

Mahadevaiah SK, Bourc'his D, de Rooij DG, Bestor TH, Turner JM, Burgoyne PS. Extensive meiotic asynapsis in mice antagonises meiotic silencing of unsynapsed chromatin and consequently disrupts meiotic sex chromosome inactivation. J Cell Biol. 2008; 182:263–276. [PubMed: 18663141]

Martin SL. The ORF1 protein encoded by LINE-1: structure and function during L1 retrotransposition. J Biomed Biotechnol. 2006; 2006:45621. [PubMed: 16877816]

Martin SL, Bushman D, Wang F, Li PW, Walker A, Cummiskey J, Branciforte D, Williams MC. A single amino acid substitution in ORF1 dramatically decreases L1 retrotransposition and provides

NIH-PA Author Manuscript

NIH-PA Author Manuscript

NIH-PA Author Manuscript

insight into nucleic acid chaperone activity. Nucleic acids research. 2008; 36:5845–5854. [PubMed: 18790804]

Martin SL, Cruceanu M, Branciforte D, Wai-Lun Li P, Kwok SC, Hodges RS, Williams MC. LINE-1 retrotransposition requires the nucleic acid chaperone activity of the ORF1 protein. Journal of molecular biology. 2005; 348:549–561. [PubMed: 15826653]

Matova N, Cooley L. Comparative aspects of animal oogenesis. Developmental biology. 2001; 231:291–320. [PubMed: 11237461]

McClellan KA, Gosden R, Taketo T. Continuous loss of oocytes throughout meiotic prophase in the normal mouse ovary. Dev Biol. 2003; 258:334–348. [PubMed: 12798292]

Moens PB, Chen DJ, Shen Z, Kolas N, Tarsounas M, Heng HH, Spyropoulos B. Rad51 immunocytology in rat and mouse spermatocytes and oocytes. Chromosoma. 1997; 106:207–215. [PubMed: 9254722]

Morita Y, Manganaro TF, Tao XJ, Martimbeau S, Donahoe PK, Tilly JL. Requirement for phosphatidylinositol-3'-kinase in cytokine-mediated germ cell survival during fetal oogenesis in the mouse. Endocrinology. 1999; 140:941–949. [PubMed: 9927327]

Morita Y, Maravei DV, Bergeron L, Wang S, Perez GI, Tsutsumi O, Taketani Y, Asano M, Horai R, Korsmeyer SJ, et al. Caspase-2 deficiency prevents programmed germ cell death resulting from cytokine insufficiency but not meiotic defects caused by loss of ataxia telangiectasia-mutated (Atm) gene function. Cell death and differentiation. 2001; 8:614–620. [PubMed: 11536012]

Morita Y, Perez GI, Paris F, Miranda SR, Ehleiter D, Haimovitz-Friedman A, Fuks Z, Xie Z, Reed JC, Schuchman EH, et al. Oocyte apoptosis is suppressed by disruption of the acid sphingomyelinase gene or by sphingosine-1-phosphate therapy. Nat Med. 2000; 6:1109–1114. [PubMed: 11017141]

O'Donnell KA, An W, Schrum CT, Wheelan SJ, Boeke JD. Controlled insertional mutagenesis using a LINE-1 (ORFeus) gene-trap mouse model. Proceedings of the National Academy of Sciences of the United States of America. 2013

O'Donnell KA, Burns KH, Boeke JD. A descent into the nuage: the maelstrom of transposon control. Developmental cell. 2008; 15:179–181. [PubMed: 18694557]

Ohno R, Nakayama M, Naruse C, Okashita N, Takano O, Tachibana M, Asano M, Saitou M, Seki Y. A replication-dependent passive mechanism modulates DNA demethylation in mouse primordial germ cells. Development. 2013; 140:2892–2903. [PubMed: 23760957]

Ollinger R, Reichmann J, Adams IR. Meiosis and retrotransposon silencing during germ cell development in mice. Differentiation. 2010; 79:147–158. [PubMed: 20227008]

Penzkofer T, Dandekar T, Zemojtel T. L1Base: from functional annotation to prediction of active LINE-1 elements. Nucleic acids research. 2005; 33:D498–500. [PubMed: 15608246]

Pepling ME, Spradling AC. Mouse ovarian germ cell cysts undergo programmed breakdown to form primordial follicles. Developmental biology. 2001; 234:339–351. [PubMed: 11397004]

Popp C, Dean W, Feng S, Cokus SJ, Andrews S, Pellegrini M, Jacobsen SE, Reik W. Genome-wide erasure of DNA methylation in mouse primordial germ cells is affected by AID deficiency. Nature. 2010; 463:1101–1105. [PubMed: 20098412]

Romanienko PJ, Camerini-Otero RD. The mouse Spo11 gene is required for meiotic chromosome synapsis. Mol Cell. 2000; 6:975–987. [PubMed: 11106738]

Schimenti J. Synapsis or silence. Nature genetics. 2005; 37:11–13. [PubMed: 15624015]

Seisenberger S, Andrews S, Krueger F, Arand J, Walter J, Santos F, Popp C, Thienpont B, Dean W, Reik W. The dynamics of genome-wide DNA methylation reprogramming in mouse primordial germ cells. Molecular cell. 2012; 48:849–862. [PubMed: 23219530]

Sharpe AH, Hunter JJ, Ruprecht RM, Jaenisch R. Maternal transmission of retroviral disease: transgenic mice as a rapid test system for evaluating perinatal and transplacental antiretroviral therapy. Proceedings of the National Academy of Sciences of the United States of America. 1988; 85:9792–9796. [PubMed: 2849117]

Sharpe AH, Jaenisch R, Ruprecht RM. Retroviruses and mouse embryos: a rapid model for neurovirulence and transplacental antiviral therapy. Science. 1987; 236:1671–1674. [PubMed: 3037694]

NIH-PA Author Manuscript

NIH-PA Author Manuscript

NIH-PA Author Manuscript

Shoji M, Tanaka T, Hosokawa M, Reuter M, Stark A, Kato Y, Kondoh G, Okawa K, Chujo T, Suzuki T, et al. The TDRD9-MIWI2 complex is essential for piRNA-mediated retrotransposon silencing in the mouse male germline. Dev Cell. 2009; 17:775–787. [PubMed: 20059948]

Sienski G, Donertas D, Brennecke J. Transcriptional silencing of transposons by piwi and maelstrom and its impact on chromatin state and gene expression. Cell. 2012; 151:964–980. [PubMed: 23159368]

Soper SF, van der Heijden GW, Hardiman TC, Goodheart M, Martin SL, de Boer P, Bortvin A. Mouse maelstrom, a component of nuage, is essential for spermatogenesis and transposon repression in meiosis. Dev Cell. 2008; 15:285–297. [PubMed: 18694567]

Sotillo R, Hernando E, Diaz-Rodriguez E, Teruya-Feldstein J, Cordon-Cardo C, Lowe SW, Benezra R. Mad2 overexpression promotes aneuploidy and tumorigenesis in mice. Cancer cell. 2007; 11:9–23. [PubMed: 17189715]

Tilly JL. Commuting the death sentence: how oocytes strive to survive. Nat Rev Mol Cell Biol. 2001; 2:838–848. [PubMed: 11715050]

Tilly JL. Ovarian follicle counts--not as simple as 1, 2, 3. Reprod Biol Endocrinol. 2003; 1:11. [PubMed: 12646064]

Toltzis P, Marx CM, Kleinman N, Levine EM, Schmidt EV. Zidovudine-associated embryonic toxicity in mice. The Journal of infectious diseases. 1991; 163:1212–1218. [PubMed: 2037787]

Trapnell C, Pachter L, Salzberg SL. TopHat: discovering splice junctions with RNA-Seq. Bioinformatics. 2009; 25:1105–1111. [PubMed: 19289445]

Trapnell C, Williams BA, Pertea G, Mortazavi A, Kwan G, van Baren MJ, Salzberg SL, Wold BJ, Pachter L. Transcript assembly and quantification by RNA-Seq reveals unannotated transcripts and isoform switching during cell differentiation. Nature biotechnology. 2010; 28:511–515.

Turner JM. Meiotic sex chromosome inactivation. Development. 2007; 134:1823–1831. [PubMed: 17329371]

Turner JM, Aprelikova O, Xu X, Wang R, Kim S, Chandramouli GV, Barrett JC, Burgoyne PS, Deng CX. BRCA1, histone H2AX phosphorylation, and male meiotic sex chromosome inactivation. Curr Biol. 2004; 14:2135–2142. [PubMed: 15589157]

Turner JM, Mahadevaiah SK, Fernandez-Capetillo O, Nussenzweig A, Xu X, Deng CX, Burgoyne PS. Silencing of unsynapsed meiotic chromosomes in the mouse. Nature genetics. 2005; 37:41–47. [PubMed: 15580272]

Wallace NA, Belancio VP, Deininger PL. L1 mobile element expression causes multiple types of toxicity. Gene. 2008; 419:75–81. [PubMed: 18555620]

Walsh CP, Chaillet JR, Bestor TH. Transcription of IAP endogenous retroviruses is constrained by cytosine methylation. Nature genetics. 1998; 20:116–117. [PubMed: 9771701]

Waterston RH, Lindblad-Toh K, Birney E, Rogers J, Abril JF, Agarwal P, Agarwala R, Ainscough R, Alexandersson M, An P, et al. Initial sequencing and comparative analysis of the mouse genome. Nature. 2002; 420:520–562. [PubMed: 12466850]

Western P. Foetal germ cells: striking the balance between pluripotency and differentiation. Int J Dev Biol. 2009; 53:393–409. [PubMed: 19412894]

Yang F, Wang PJ. The mammalian synaptonemal complex: a scaffold and beyond. Genome dynamics. 2009; 5:69–80. [PubMed: 18948708]

Zemojtel T, Penzkofer T, Schultz J, Dandekar T, Badge R, Vingron M. Exonization of active mouse L1s: a driver of transcriptome evolution? BMC Genomics. 2007; 8:392. [PubMed: 17963496]

Zheng Q, Wang XJ. GOEAST: a web-based software toolkit for Gene Ontology enrichment analysis. Nucleic acids research. 2008; 36:W358–363. [PubMed: 18487275]

NIH-PA Author Manuscript

NIH-PA Author Manuscript

NIH-PA Author Manuscript

Highlights

- Differential nuclear retrotransposon L1 levels in meiotic prophase I fetal oocytes
- Increased L1 expression precipitates oocyte genome damage and meiotic defects
- AZT implicates RNA/DNA hybrids in triggering oocyte death and chiasma failure
- L1 activity underlies fetal oocyte attrition, reduced ovarian reserves and aneuploidy

NIH-PA Author Manuscript

NIH-PA Author Manuscript

NIH-PA Author Manuscript

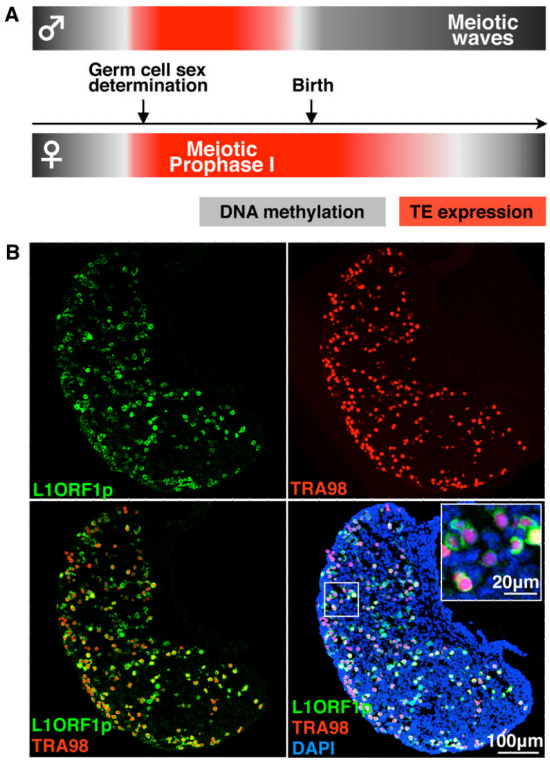

Figure 1. L1 Expression in Meiotic Prophase I Fetal Oocytes

(A) Meiotic prophase I in oocytes coincides with epigenetic reprogramming of the germ cell genome and activation of retrotransposon expression.

(B) Single and merged channels of single confocal sections of E18.5 WT ovary showing L1ORF1p (green) expression in TRA98-positive (red) fetal oocytes counterstained with DAPI (blue).

See also Figure S1.

NIH-PA Author Manuscript
NIH-PA Author Manuscript
NIH-PA Author Manuscript

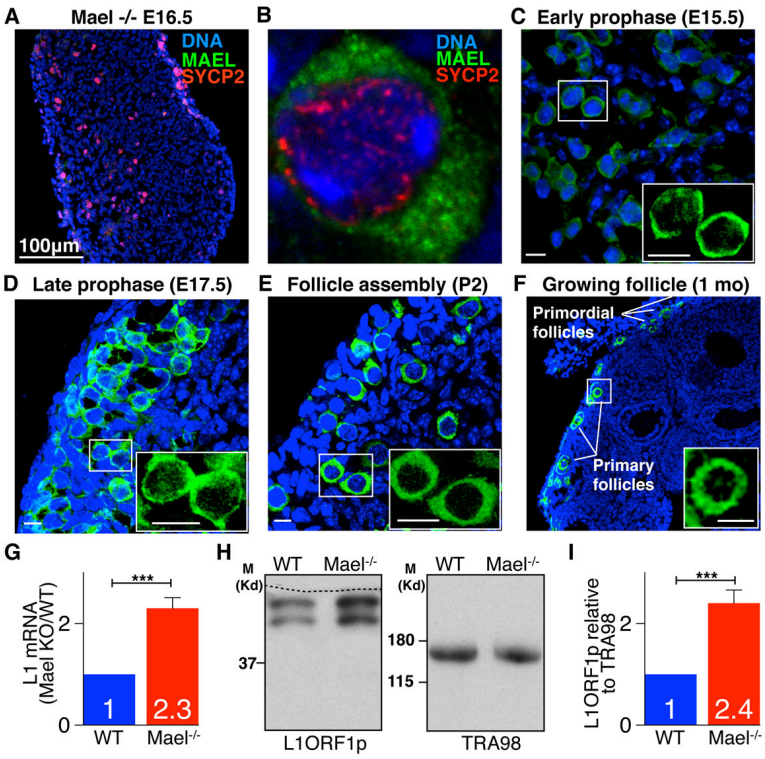

Figure 2. MAEL is Required for L1 Regulation in Fetal Ovaries

(A) Section of E16.5 *Mael*-mutant ovary section probed with MAEL antibody.

(B) Cytoplasmic MAEL (green) localization in WT E15.5 oocytes. SYCP2 (red) marks chromosome axes.

(C–F) WT ovaries of indicated developmental stages and ages probed with MAEL antibody. MAEL expression is observed in fetal oocytes throughout meiotic prophase I and in primordial, and primary follicles. Insets - MAEL single channel (green) close-up views. Bars represent 10 μm.

(G) qRT-PCR analysis of L1 mRNA levels relative to expression of germ cell-specific *Mvh*. (Mean ± St.dev. from three independent measurements are shown, t=10.82, p=0.0004). (H) Western blot detection of L1ORF1p relative to TRA98 expression in E15.5 ovaries based on results of analysis of three biological replicates. Dashed line marks the cut line of the membrane. (I) Quantification of Western blot data shown in (H). (Mean ± St.dev. from three independent measurements are shown, t =9.31, p=0.0007). Two-tailed unpaired Student's t-test, ***-P<0.001 (G, I).

See also Figure S2 and Table S1.

NIH-PA Author Manuscript

NIH-PA Author Manuscript

NIH-PA Author Manuscript

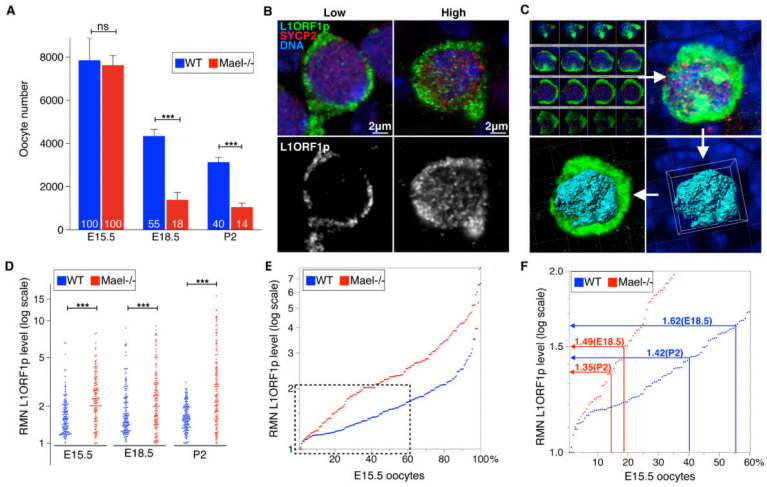

Figure 3. Viability of Wild-type and *Mael*-null Oocytes Correlates with Nuclear L1ORF1p Levels

(A) Quantification of WT and *Mael*-null oocytes. Mean ± St.dev. from at least three independent measurements are shown (two-tailed unpaired Student's t-test, ns-P>0.05; ***-P<0.001).

(B) Variable (low and high) nuclear L1ORF1p levels (green) in E15.5 WT oocytes. SYCP2 (red) marks the synaptonemal complex.

(C) Representation of 3D reconstruction from single confocal sections, and generation of the nuclear surface (cyan) within which green signal intensity is quantified to determine L1ORF1p RMN levels in oocyte nuclei using Imaris Software.

(D) Dot-plot of RMN L1ORF1p levels in WT and *Mael*-null oocytes (two-tailed Kolmogorov-Smirnov test, ***-P<0.001).

(E) E15.5 WT and *Mael*-null oocytes ranked according to their RMN L1ORF1p levels.

(F) Chart relating RMN L1ORF1p levels in WT and *Mael*-null E15.5 oocytes to percentage of their survival to E18.5 and P2. Boxed area in (E) is shown in detail in (F).

See also Table S2.

NIH-PA Author Manuscript

NIH-PA Author Manuscript

NIH-PA Author Manuscript

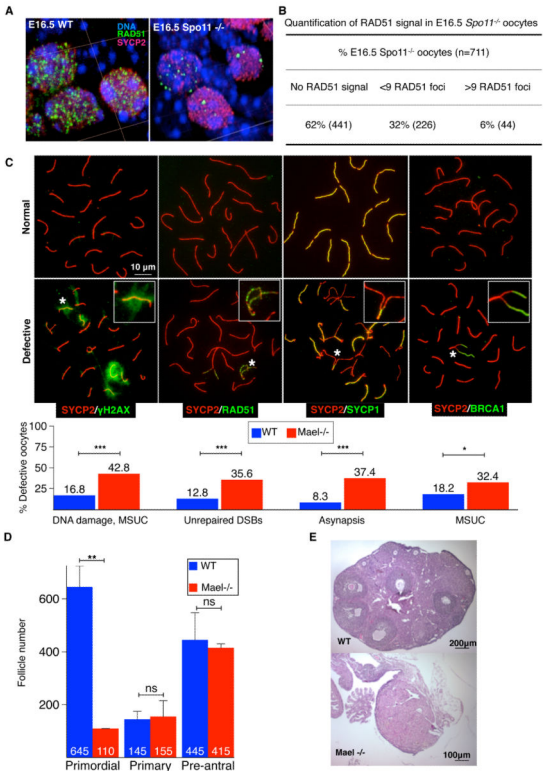

Figure 4. Non-meiotic DSBs and Meiotic Prophase I Defects in Fetal Oocytes

(A) A 3D-rendered image of a section of a WT and *Spo11*-null E16.5 ovary immunostained for RAD51 (green) and SYCP2 (red).

(B) Quantification of RAD51 foci in *Spo11*-null E16.5 oocytes.

(C) Representative images of pachytene meiotic spreads and quantification of defective patterns of DNA damage, DNA repair, synapsis and MSUC, assessed respectively with γH2AX, RAD51, SYCP1, BRCA1 antibodies (green). SYCP2 (red) marks synaptonemal complex lateral elements. Insets – close-ups of abnormal patterns indicated with asterisks. (Two-tailed Fisher's exact test, *-P<0.05; ***-P<0.001).

(D) Follicle counts in P19 WT and *Mael*$^{-/-}$ ovaries. Lack of primordial follicles is apparent in P19 *Mael*-mutant ovaries. No effect of *Mael* deletion is observed on the number of primary and pre-antral follicles. Mean ± St.dev. from at least three independent biological measurements are shown (two-tailed unpaired Student's t-test, ns-P>0.05; **-P<0.01).

(E) Hematoxylin/Eosin-stained sections of ovaries of a 1 year-old WT and *Mael*$^{-/-}$ females.

See also Figure S3 and Tables S3 and S4.

NIH-PA Author Manuscript

NIH-PA Author Manuscript

NIH-PA Author Manuscript

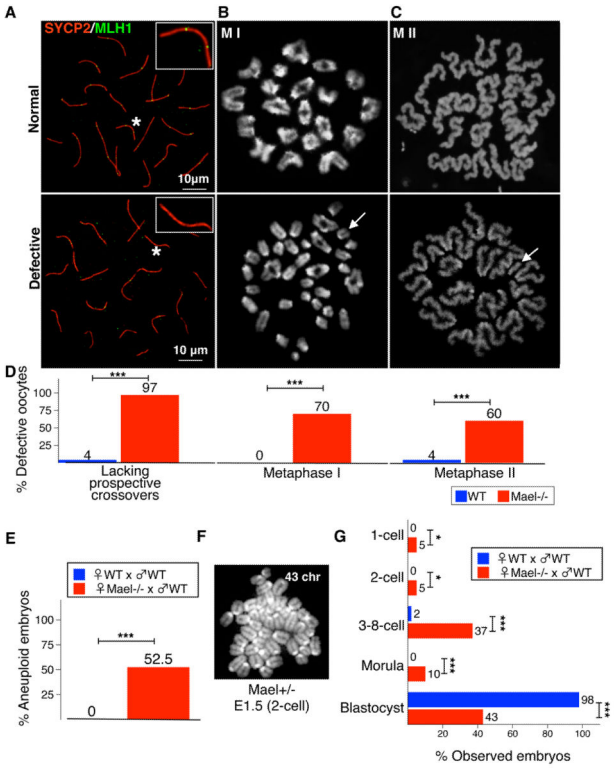

Figure 5. Crossover Defects, Aneuploidy and Premature Ovarian Oocyte Depletion in the *Mael*-null Mutant

(A) Representative images and quantification of prospective crossovers identified using MLH1 antibody (green) in WT and *Mael*-null E18.5 pachytene nuclei. Insets - close-up views of synaptonemal complexes (identified with asterisks) with two and none MLH1 foci.

(B, C) Representative images and quantification of karyotypes in metaphase I and metaphase II WT and *Mael*-null oocytes. Arrow in defective MI oocyte (B) identifies one of 30 chromosomal univalents present in this sample. Arrow in defective MII oocyte (C) identifies a single extra chromosome.

(D) Quantification of defective oocytes in (A–C).

(E) Quantification of aneuploid karyotypes of 2-cell embryos obtained from *Mael*-null and control WT oocytes.

(F) Representative image of an aneuploid karyotype (43 chromosomes) of an E1.5 $Mael^{+/-}$ embryo.

(G) Staging of $Mael^{+/-}$ embryos developed from *Mael*-null oocytes and control WT embryos collected at E3.5 (1C - 1-cell, 2C - 2-cell, 3-8C - 3- to 8-cell arrested embryos, M - Morula, and B - Blastocyst). Two-tailed Fisher's exact test, ns-P>0.05; **-P<0.01, ***-P<0.001 (D, E and I).

See also Figure S4 and Tables S4 and S5.

NIH-PA Author Manuscript

NIH-PA Author Manuscript

NIH-PA Author Manuscript

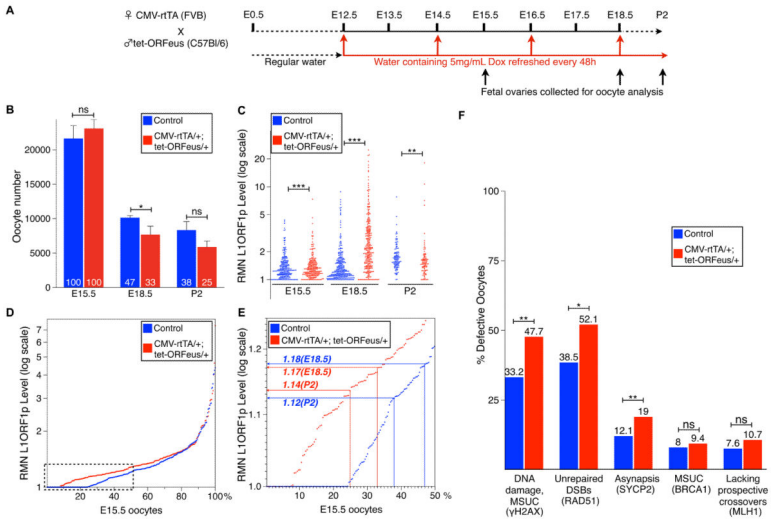

Figure 6. Effects of Doxycycline-inducible tet-*ORFeus* Expression on Fetal Oocytes

(A) Diagram of experimental induction of tet-*ORFeus* expression.

(B) Quantification of oocytes in doxycycline-induced non-double transgenic control and CMV-rtTA/+; tet-*ORFeus*/+ embryos. Mean ± St.dev. from at least three independent biological measurements are shown (two-tailed unpaired Student's t-test, ns-P>0.05; *-P<0.05; ***-P<0.001).

(C) Dot-plot of RMN L1ORF1p levels in non-double transgenic control and CMV-rtTA/+; tet-*ORFeus*/+ doxycycline-induced oocytes. Each dot represents the RMN level in an individual oocyte nucleus. (two-tailed Kolmogorov-Smirnov test, *-P<0.05; **-P<0.01; ***-P<0.001).

(D) E15.5 non-double transgenic control and CMV-rtTA/+; tet-*ORFeus*/+ oocytes ranked according to their RMN L1ORF1p levels. Boxed area is shown in detail in (E).

(E) Chart relating RMN L1ORF1p levels in non-double transgenic control and CMV-rtTA/+; tet-*ORFeus*/+ E15.5 oocytes to percentage of their survival to E18.5 and P2.

(F) Quantification of E18.5 non-double transgenic control and CMV-rtTA/+; tet-*ORFeus*/+ doxycycline-induced oocytes exhibiting evidence of DNA damage and MSUC (by γH2AX staining), persistent DSBs (by RAD51 foci), asynapsis (by abnormal SYCP2 staining), MSUC (by BRCA1 staining) and lacking MLH1 foci. (Two-tailed Fisher's exact test, ns-P>0.05; *-P<0.05; **-P<0.01).

See also Figure S3 and Tables S3 and S6.

NIH-PA Author Manuscript
NIH-PA Author Manuscript
NIH-PA Author Manuscript

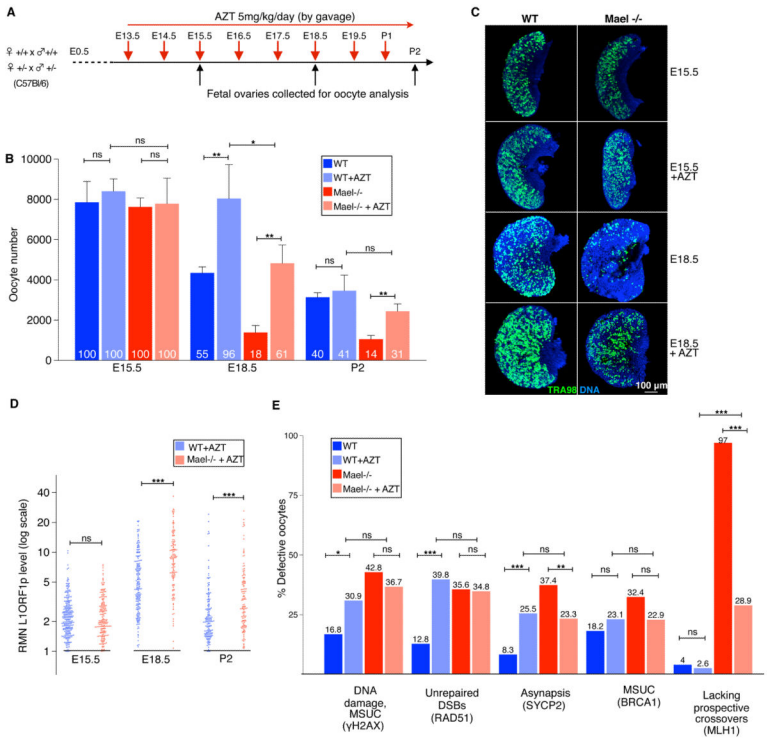

Figure 7. Fetal Oocyte Attrition and Meiotic Prophase I Progression in AZT-treated Mice

(A) Diagram of AZT treatment of pregnant WT and *Mael*+/− mutant females.

(B) Quantification of untreated and AZT-treated WT and *Mael*-null oocytes. Mean ± St.dev. from at least three independent measurements are shown (two-tailed unpaired Student's t-test, ns-P>0.05; ***-P<0.001; ** - P<0.01, *-P<0.05).

(C) Whole mount TRA98 (green) labeling of fetal oocytes in untreated and AZT-treated WT and *Mael*-null ovaries.

(D) Dot-plot of RMN L1ORF1p levels in AZT-treated WT and *Mael*-null oocytes (two-tailed Kolmogorov-Smirnov test, ns-P>0.05, ***-P<0.001).

(E) Quantification of untreated and AZT-treated WT and *Mael*-null E18.5 oocytes exhibiting evidence of DNA damage and MSUC (by γH2AX staining), persistent DSBs (by RAD51 foci), asynapsis (by abnormal SYCP2 staining), MSUC (by BRCA1 staining) and lacking MLH1 foci. (Two-tailed Fisher's exact test, ns-P>0.05; ***-P<0.001; ** - P<0.01, *-P<0.05).

See also Figures S3 and S5, and Tables S3 and S7.